Colloid & Polymer Science Colloid Polym Sci 270:455–464 (1992)

Deformation behavior of oriented UHMW-PE fibers

L. E. Govaert and P. J. Lemstra

Centre for Polymers and Composites, Eindhoven University of Technology, Eindhoven, The Netherlands

Abstract: The mechanical behavior of gel-spun, ultra-drawn, UHMW-PE fibers was investigated as a function of temperature, stress, and time under static and dynamic loading conditions. From a phenomenological point of view, two separate contributions to the deformation behavior could be distinguished, i.e., a reversible (viscoelastic) contribution and an irreversible plastic flow component. It was investigated whether or not this distinction can be rationalized on a molecular basis. The fibers were studied using static (creep) and dynamic mechanical analysis (DMA), dilatometry, and wide-angle x-ray scattering (WAXS). The results of the combined experimental observations are discussed in an attempt to relate the deformation behavior of highly oriented PE fibers to events occurring on a molecular scale.

Key words: Polyethylene; fibers; structure; dynamic behavior; volume expansion

Introduction

Many routes have been developed to obtain a high degree of orientation and chain-extension in fibrous polyethylene systems [1–3]. A technologically useful method to obtain highly oriented/chain-extended fibers, based on ultra-high molecular weight polyethylene (UHMW-PE), is the so-called gel-spinning/drawing process [4]. UHMW-PE fibers produced by this process are at present commercially available and possess moduli and strength levels up to 170 GPa and 4 GPa, respectively. However, intrinsically, the performance of PE fibers is less impressive with respect to high temperatures or long-term loadings, and, consequently, there has been considerable interest in the time-dependence of the deformation behavior of these fibers.

In the case of melt-spun/drawn polyethylene fibers, Wilding and Ward [5–7] followed a phenomenological approach, where the total deformation is considered to originate from a reversible, linear viscoelastic (delayed elastic) contribution and a non-linear plastic flow component [5]. Recently, we applied this phenomenological approach to describe the deformation behavior of gel-spun UHMW-PE fibers [8]. It was shown that separate characterization of the reversible viscoelastic and the irreversible flow contribution leads to a phenomenological stress-strain relation that is in good accordance with the actual fiber behavior under various loading conditions over a broad range of frequencies (loading times) and temperatures [8].

The question arises whether the phenomenological distinction between reversible and irreversible contributions to the deformation of highly oriented polyethylene fibers can be rationalized on a molecular basis. The Irvine/Smith model [9] predicts a unique modulus vs. draw ratio curve based on a simple two-phase model of, respectively, an oriented crystalline (helix, in their terminology) and amorphous fraction (coil). Another two-phase model, in terms of crystalline and amorphous orientation functions was presented by Anandakumaran et al. [10], who pointed out the pronounced influence of the amorphous orientation on the tensile modulus of oriented polyethylene. In an attempt to elucidate the nature of the "amorphous" component in oriented polyethylene, Deckmann et al. studied oriented polyethylene fibers using NMR [11]. It was shown that different motional states could be distinguished, related to a

crystalline fraction that is perfectly oriented, but partly mobile and a non-crystalline fraction that is oriented to some extent [11]. The motional state of the mobile crystalline fraction is governed by a fast exchange of gauche defects, the non-crystalline fraction is dynamically disordered as a consequence of segmental motion [11].

In this study, the results of static and dynamic mechanical experiments, wide-angle x-ray scattering (WAXS), dilatometry, constrained and unconstrained heating are combined with literature data in an attempt to describe the involvement of crystalline and non-crystalline components in the reversible and irreversible deformation processes in oriented PE structures. The authors hasten to add that it is not intended to propose another model for the structure of oriented polyethylene, in view of the abundance of models in literature [12], but the purpose of this paper is merely to relate the *dynamic* stress-strain behavior of oriented PE fibers, in terms of reversible and irreversible deformation, to events occurring on a molecular scale.

Experimental

A) *Materials*

All experiments, unless stated otherwise, have been performed on gel-spun ultra-drawn UHMW-PE fibers Dyneema SK66, supplied by DSM-HPF as a multi-filament yarn of 1600 den. The modulus and strength of the fibers were 85 GPa and 3 GPa, respectively.

To study the effect of irreversible creep deformation on the tensile modulus of oriented PE, experiments were performed on partially drawn UHMW-PE fibers of 50 den. These 50 den fibers were spun from a 10 wt.-% UHMW-PE solution and possessed, after partial drawing, a tensile modulus of approx. 50 GPa. The UHMW-PE grade used for both fibers possessed a weight average molecular weight of approx. $2\,10^3$ kg/mole.

For comparative experiments, solution-crystallized/drawn tapes with a draw-ratio of 40 were used. The tapes were obtained by casting films from 2 wt.-% UHMW-PE solutions of the same grade. After casting, see also the experimental section of reference [4], the solvent was evaporated at room temperature. The resulting dry films were cut into pieces of 50 $\times$ 10 mm^2 and drawn at 120 °C to a draw ratio of 40, resulting in tapes possessing tensile moduli of approx. 60 GPa.

B) *Techniques*

Thermorheological behavior: The thermorheological behavior of the reversible part of the deformation was studied in dynamic mechanical and stress relaxation experiments at low strain levels (reversible deformation). Dynamic experiments were performed in uniaxial extension in the frequency range from 0.2 to 3 Hz, at temperatures from -20 to 105 °C [8]. The equipment used for the experiments was a Polymer Laboratories DMTA MK2. By splitting the multi-filament yarn, samples were prepared with a reduced cross-sectional area of 0.01 mm^2 and a length of 20 mm. To improve clamping, the fiber ends were provided with cardboard tabs, glued together with an epoxy resin.

Stress relaxation experiments were performed at a strain of 0.5% (reversible deformation) at temperatures from 30° to 70 °C on a Frank 81565 tensile tester equipped with an extensometer and a thermostatically controlled oven.

The temperature dependence of the plastic flow contribution was analyzed in terms of the plateau creep rate [8]. Creep experiments were performed in dead-weight loading at stress levels ranging from 200 to 1000 MPa and temperatures from 30° to 90 °C [8]. The strain was monitored as a function of time, whereas the plateau creep rate was subsequently determined by plotting the strain rate logarithmically vs. strain in so-called Sherby-Dorn plots [8, 13]. For both the stress relaxation and creep experiments, fiber samples of 255 mm length were used, provided with cardboard tabs to improve clamping.

Volume expansion (WAXS, dilatometry): The temperature dependence of the orthorhombic unit cell volume was monitored by measuring the unit cell dimensions (a-, b-, c-axis) using wide-angle x-ray equipment, a Siemens D500TT diffractometer, and Ni-filtered Cu K_α-radiation ($\lambda = 1.5406$ Å) with a graphite monochromator. The scans were performed on 2.5-cm long pieces of yarn, positioned in a special holder between aluminum foil. For the 200, 110, 020, and 310 reflections, the fiber axis was directed perpendicular to the 2θ-scanning plane. The 2θ-scan was performed from 19 to 46° (2θ) with steps of 0.02°, each step being monitored for 10 s. For the 002 reflection the fiber axis was directed parallel to the scanning plane. This 2θ-scan was performed from 73° to 76° (2θ) with steps of 0.02°, where again each step was monitored for 10 s.

The dimensions of the a-, b-, and c-axis were calculated from the 200, 020, and 002 reflections, respectively [14]. The calculated dimensions were cross-checked on the 110 and 310 reflections, showing deviations less than 0.1%.

The temperature dependence of the total fiber volume was monitored with dilatometry using mercury as the confining liquid. The dilatometer used in this study has been described in detail elsewhere [15]. The total volume of the cell was about 15 ml. The volume change was measured with a capillary of 50 cm and an inner diameter of about 1.5 mm. The instrument was calibrated with mercury, using a volume expansion coefficient of $1.82\,10^{-4}\,K^{-1}$ for mercury [16] in the experimentally covered temperature range of 25° to 120 °C. The experiments were performed on the 1600 den fiber and on solution-crystallized/drawn tapes with a draw ratio of 40. For each experiment about 1 g of material was used. The confining liquid, mercury, was added under a high vacuum (10^{-5} torr). The filled dilatometer was heated stepwise in a thermostatically controlled oilbath from 25° up to 120 °C. After each temperature step an equilibration time of 20 min was allowed. The temperature was measured with an accuracy of 0.1 °C, the volume change was monitored with an accuracy of 0.00185 ml/division.

Thermal shrinkage and retractive stress: Thermal shrinkage was monitored using a Frank 81565 tensile tester equipped

with an extensometer and a thermostatically controlled oven. The fibers (SK66) were clamped and a weight of 50 g (2.6 MPa) was attached to supply the small pre-tension needed for proper use of the extensometer. The shrinkage strain could be monitored with an absolute accuracy of about 0.002%. The experiment was started at 30 °C and, subsequently, the temperature was increased in steps of 5 °C. After each step an equilibration time of 15 min was allowed before the shrinkage was measured.

The retractive stress, or shrinkage stress, was measured on a Frank 81565 tensile tester equipped with a thermostatically controlled oven. The fibers were strained to an initial load of 10 MPA at 30 °C and kept at a constant strain level. Subsequently, the sample was heated at a heating rate of about 8 °Cmin^{-1}. During heating, the retractive force was monitored as a function of temperature. Stress and temperature were measured with an accuracy of 1% and 0.1 °C, respectively.

Stiffening effects: reversible and irreversible deformation: To investigate the influence of reversible deformation on the dynamic modulus of the polyethylene fiber (SK66), experiments were performed on a Zwick Rel servo hydraulic tensile tester (20 kN), adapted for low frequency noise strain excitation. The samples, used for these experiments, were 255 mm long, and provided with cardboard tabs to improve clamping. In the experiments, the samples were loaded at room temperature to a static strain level in the range of 0.25 to 1.75%. The total loading time at high strain levels (above 1.0%) did not exceed 20 min, which excludes any irrecoverable (plastic flow) contribution to the deformation [8]. Subsequently, a low-frequency noise signal, 256 frequencies in the range of 0 to 10 Hz, was used to superimpose a dynamic strain, with an amplitude of 0.05%, on the statically loaded fibre. Stress output and strain input were transformed into dynamic quantities in the frequency range from 0.5 to 5 Hz using a HP 98785A Fast Fourier Analyzer.

The sonic modulus of SK66 yarn was monitored during a reversible creep experiment. The experiments were performed on equipment of AKZO Corporate Research (Arnhem, The Netherlands), described in detail in the experimental section of [17]. A piece of yarn of 2.5 m was loaded at room temperature at a low stress level (100 MPa) to ensure complete reversibility of the resulting deformation [8]. The creep of the yarn was measured with an inductive displacement transducer, which was positioned about 2 m from the clamp. The sonic velocity was measured at 1 min intervals for 20 min. The fiber was subsequently unloaded and the experiment was repeated after a recovery period of 1.5 h. The sonic modulus E_s of the fiber was determined using the equation $E_s = \rho c^2$, where ρ is the density of the material and c is the longitudinal wave velocity, or sonic velocity.

To investigate the influence of irrecoverable deformation on the tensile modulus, samples of the 50 den fiber were loaded in creep at 300 MPa and 50 °C for periods varying from a few hours up to 2 weeks. The samples were provided with cardboard tabs and had a length of 100 mm. After unloading, the samples were allowed to recover for a period of 1 week at 50 °C. Using the cardboard tabs as a reference, the irrecoverable deformation of each sample was measured. Subsequently, the moduli of the samples were determined in tensile testing at 30 °C and a strain rate of 0.001 s^{-1}.

Results

Deformation behavior: dependence on stress and temperature

The main results concerning the mechanical and thermorheological behavior of oriented PE fibers, partly published elsewhere [8], will be recapitulated and updated.

Figure 1a shows the creep compliance ($= \varepsilon(t)/\sigma$) of oriented polyethylene (Dyneema SK66) as a function of temperature and at various loadings. As shown previously [8], the deformation behavior of oriented polyethylene can be considered to be the resultant of two simultaneous contributions:

1) a reversible (visco-elastic), nearly stress-linear process which dominates at short loading times, low temperatures and/or low stress levels;
2) a non-linear plastic flow contribution which becomes more pronounced at longer loading times, high temperatures and high stress levels.

The *reversible* contribution can be determined independently from stress relaxation experiments at low strain levels (0.5%) [18]. From these data, the reversible contribution to the creep deformation was predicted [18]. By substracting this contribution from the total deformation, the plastic flow contribution is revealed as shown in Fig. 1b.

In order to test the thermorheological behavior of oriented PE fibers, both DMTA and stress relaxation experiments were performed at low strain levels (reversible deformation) [8]. DMTA experiments were performed in the frequency range of 0.2 to 3 Hz at temperatures from -20 to 105 °C [8]. Master curves of the dynamic quantities E_d and tan δ could be obtained using only a horizontal shift $a_{T0}(T)$ [8]. The shift factor $a_{T0}(T)$ was also determined from stress relaxation experiments at 0.5% strain in the time range from 100 to 10 000 s. The Arrhenius plot of the shift factors $a_{T0}(T)$, as derived from the dynamic and the stress relaxation experiments, is presented in Fig. 2a [8].
Two important observations can be made:

1) The observed temperature dependence cannot be described by a single, temperature activated Arrhenius process. The apparent activation energy on the lower temperature scale, up to about 50 °C, is approx. 30 kcal/mol, but increases gradually with increasing temperature

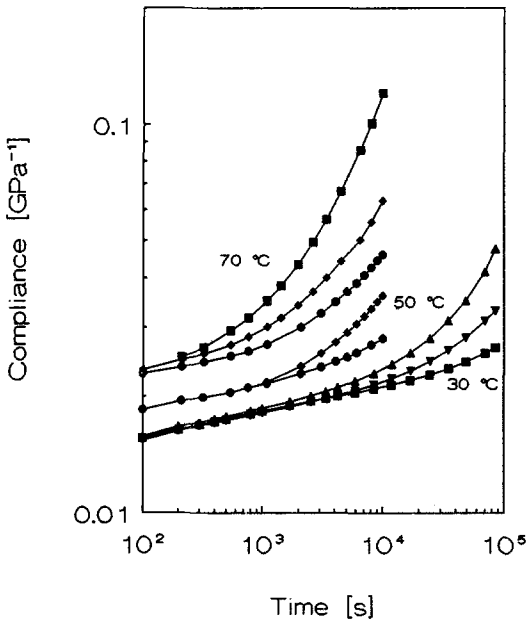

Fig. 1a. Creep compliance of a gel-spun, ultra-drawn UHMW-PE fiber (SK66) at various temperatures and loads; 250 MPa (●), 400 MPa (◆), 500 MPa (■), 750 MPa (▼) and 1 GPa (▲).

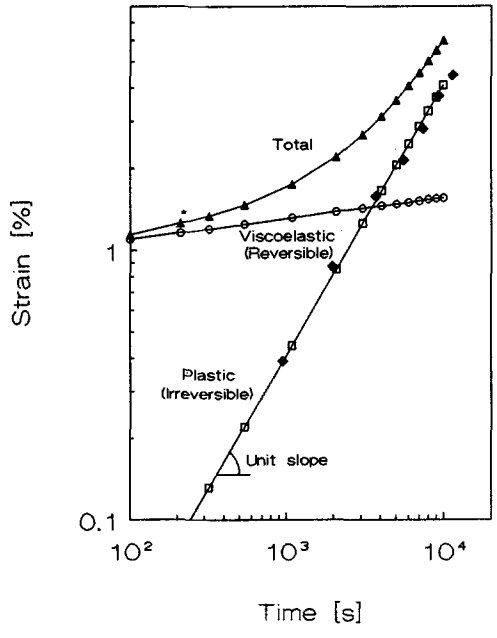

Fig. 1b. Creep deformation of a gel-spun, ultra-drawn UHMW-PE fibers (SK66) at 70 °C and a load of 500 MPa (▲), decomposed into a viscoelastic power law creep (○) and a plastic, continuous flow process (□). Experimental data on irrecoverable deformation are represented by (◆).

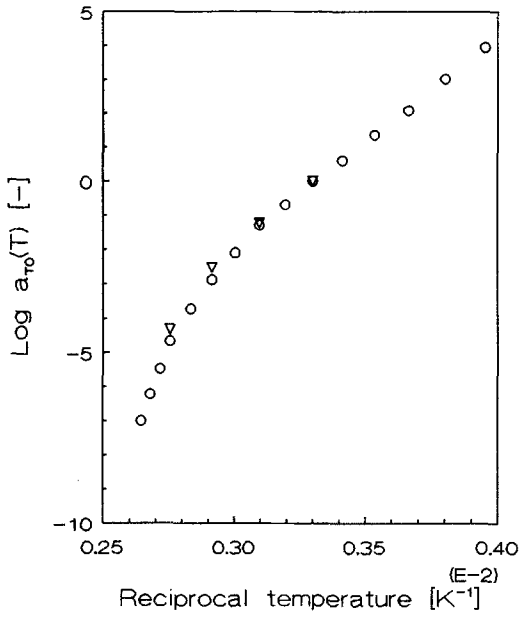

Fig. 2a. Arrhenius plot of the temperature dependence of the shift factor $a_{T0}(T)$ of the reversible contribution to the deformation for a reference temperature of 30 °C. (○): Shift factor derived from dynamic experiments in the range of 0.2 to 5 Hz. (▽): Shift factor as derived from stress relaxation experiments at 0.5% strain.

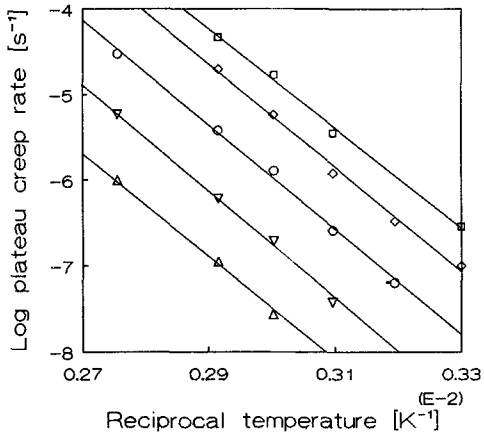

Fig. 2b. Arrhenius plot of the plateau creep rate (plastic flow contribution) at various stress levels; 200 MPa (△), 300 MPa (▽), 500 MPa (○), 750 MPa (◇), and 1 GPa (□).

to physically unrealistic values of approx. 100 kcal/mol;

2) The temperature dependence of the shift factor, as derived from stress relaxation experiments, agrees with the temperature dependence of the shift factor as derived from the dynamic quantities.

The *plastic* flow contribution was analyzed via long-term creep experiments at various stress levels and temperatures [8]. From the creep data, the plastic flow contribution (plateau creep rate) was determined by employing the method suggested by Sherby and Dorn [13]. The Arrhenius plot of the plateau creep rate is presented in Fig. 2b. The temperature dependence of the plastic flow contribution, Fig. 2b, appears to be independent of the applied stress. Moreover, the Arrhenius plot of the plateau creep rate can be approximated by a straight line, which indicates that, within the temperature range that is covered experimentally, the plastic flow contribution originates from a single, thermally activated, Arrhenius process. The activation energy of this process, as derived from Fig. 2b, is approx. 30 kcal/mol.

Volume expansion: WAXS vs dilatometry

In order to determine the volume/temperature behavior of the "amorphous" fraction, the volume expansion of the crystalline fraction was measured using WAXS and compared with the total specific volume expansion of the fibers measured by dilatometry.

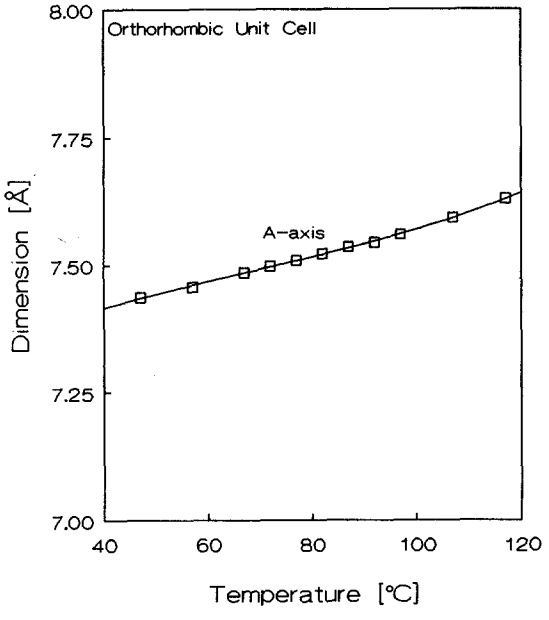

Fig. 3a. Dimension of the a-axis of the orthorhombic unit cell as a function of temperature (WAXS).

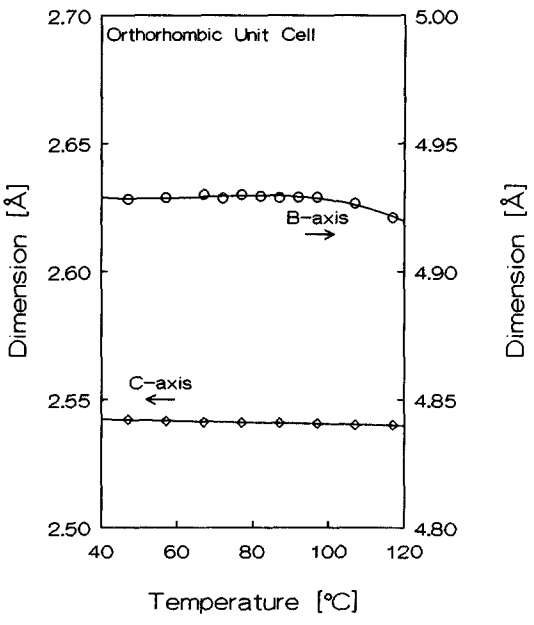

Fig. 3b. Dimensions of the b- and c-axis of the orthorhombic unit cell as a function of temperature (WAXS).

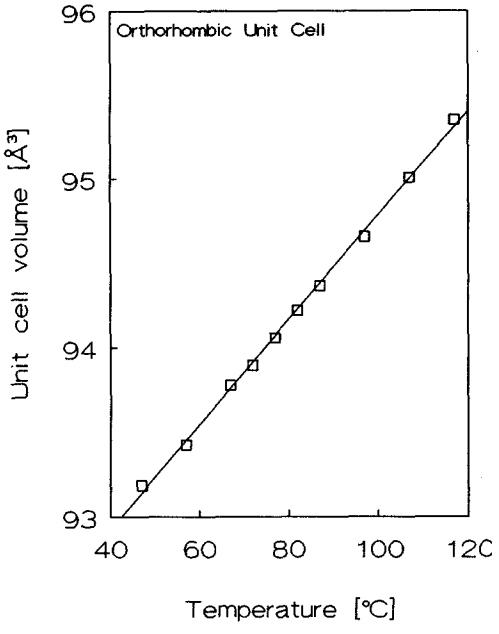

Fig. 4. Volume of the orthorhombic unit cell as a function of temperature, as derived from the data in Figs. 3a and b.

The WAXS results for the temperature dependences of the dimensions of the a-, b-, and c-axis of the orthorhombic unit cell are presented in Figs. 3a and b. The unit cell volume is determined by multiplication of the a-, b-, and c-dimensions.

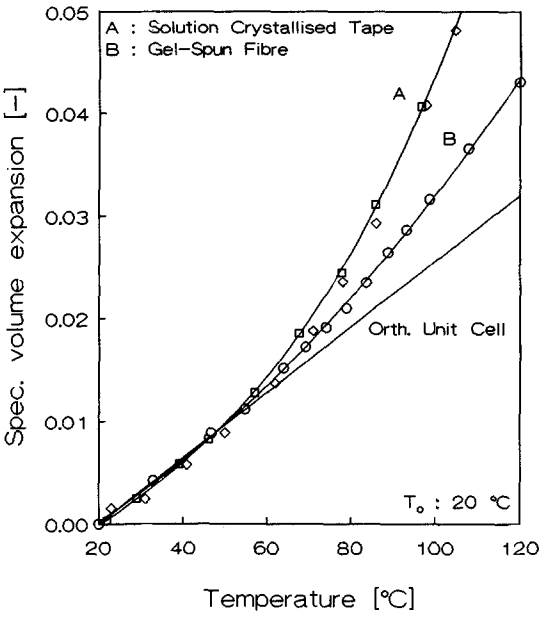

Fig. 5. Specific (total) volume expansion of gel-spun fiber (○) and solution crystallized/drawn tapes (□: first run; ◇: second run). The straight line represents the specific volume expansion of the orthorhombic unit cell (taken from Fig. 4).

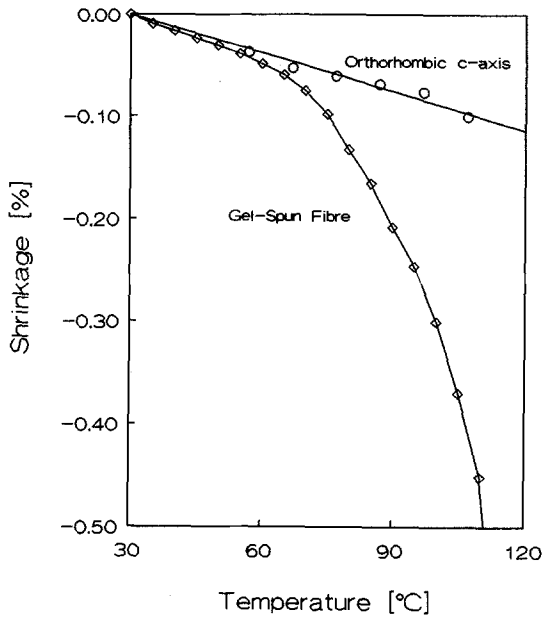

Fig. 6. Shrinkage of gel-spun fiber (SK66)upon unconstrained heating (◇), compared with shrinkage of the c-axis of the orthorhombic unit cell (○).

The resulting data are presented in Fig. 4. An approximately linear volume expansion of the orthorhombic unit cell is observed, with a linear volume expansion coefficient α_v of 3.33 10^{-4} K^{-1}. This volume expansion coefficient is used in Fig. 5 to compare the specific unit cell expansion with the specific total volume expansion measured via dilatometric experiments on the gel-spun fiber SK66 and the solution-crystallized/drawn tapes. As is evident from Fig. 5, the total volume of the gel-spun fiber increases non-linearly with temperature, and deviates markedly from the volume expansion of the orthorhombic unit cell. For the less crystalline solution-crystallized/drawn tapes this behavior is even more pronounced. Upon temperature-recycling of the experiments, the volume expansion behavior appears to be reversible.

Thermal shrinkage and retractive stress

The SK66 yarn was subjected to unconstrained and constrained heating experiments. Upon unconstrained heating, where the fiber is allowed to contract freely, the gel-spun fiber initially shows a linear shrinkage with temperature (Fig. 6). The linear thermal expansion coefficient of $-15.6\ 10^{-6}\ K^{-1}$ is slightly higher than the value found for the orthorhombic c-axis (Fig. 3b, $-12.6\ 10^{-6}\ K^{-1}$). Above 60 °C, the shrinkage behavior of the fiber increases drastically and deviates markedly from the shrinkage of the orthorhombic c-axis.

In constrained heating (Fig. 7), i.e. at fixed length, a gradual increase of the retractive stress is observed. At a temperature of 135 °C the retractive stress reaches its maximum value, and decreases with increasing temperature. These observations are similar to those reported before for both melt-spun/drawn [19–20] and gel-spun/drawn PE fibers in current literature [21].

Stiffening effects: reversible and plastic flow deformation

The effect of reversible deformation on the dynamic modulus (1 Hz, room temperature) of the Dyneema SK66 yarn is shown in Fig. 8. The dynamic modulus is found to increase significantly with increasing strain. This increase appears to be instantaneous, and is approximately independent of the loading time. The stiffening effect is also observed when monitoring the sonic modulus of the yarn during reversible creep deformation, as

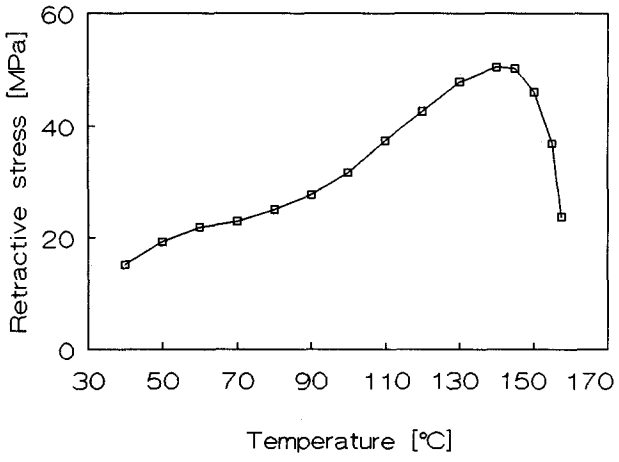

Fig. 7. Reactive stress of gel-spun fiber (SK66) upon constrained heating.

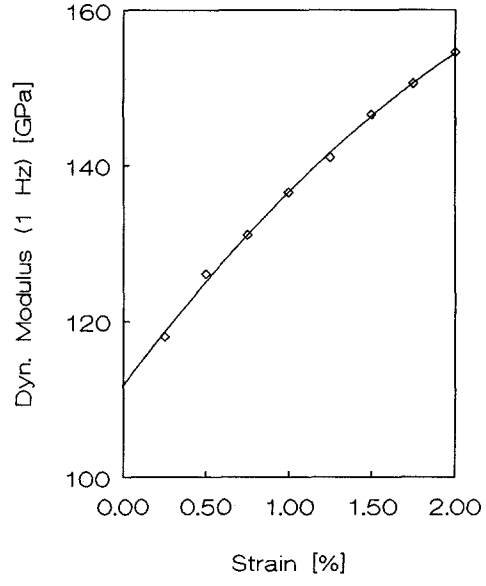

Fig. 8. Dynamic modulus E_d, measured at 1 Hz, of gel-spun UHMW-PE yarn (SK66) as a function of statically applied reversible strain (reversible effects).

shown in Fig. 9. A gradual increase of the sonic modulus with increasing strain (loading time) is observed. Moreover, upon second loading the reversibility of this effect is evident. The observations are in accordance with the results of Khanna et al. [22], who called this phenomenon elastic orientation under force (EOF).

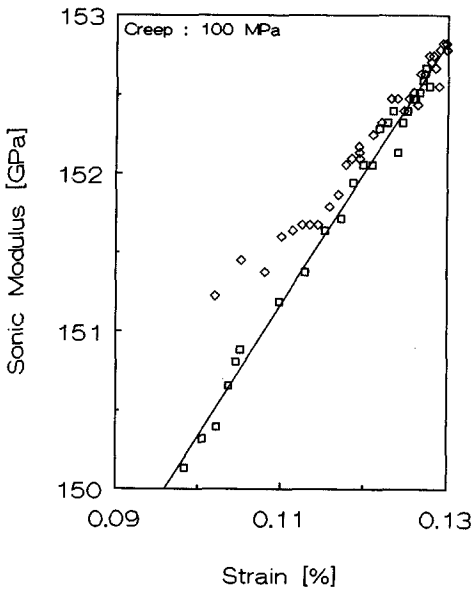

Fig. 9. Sonic modulus of gel-spun UHMV-PE fiber (SK66) as a function of creep deformation at a load of 100 MPa (reversible deformation). (□): first run, (◇): second run after 1.5 h recovery.

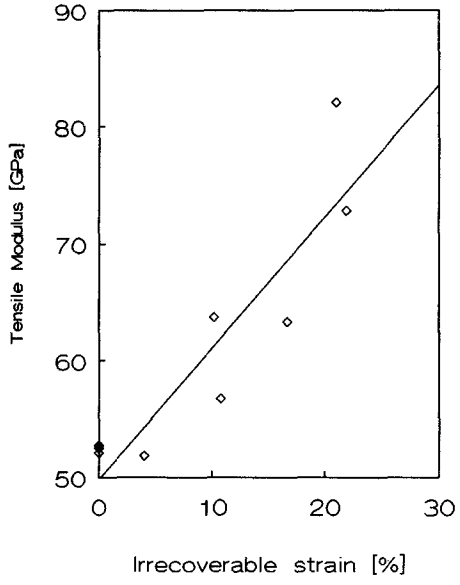

Fig. 10. Tensile modulus of gel-spun UHMW-PE fiber (50 den) as a function of irrecoverable deformation (◇).

The influence of plastic flow deformation on the tensile modulus of gel-spun UHMW-PE fibers is depicted in Fig. 10. A significant increase in the tensile modulus is observed with increasing plastic creep deformation.

Discussion

Irreversible deformation (plastic flow)

The assignment of the irreversible deformation is relatively straightforward. In the case of plastic flow, a fast molecular movement has to be involved, since the material has to remain in an equilibrium state with respect to the rate of deformation. The fast exchange of gauche defects that is observed with solid state NMR in the crystalline fraction [11] seems to meet this requirement. Recent results of molecular dynamics simulations show that the exchange of gauche defects could be as fast as $10^{10}\ s^{-1}$, whereas the lifetime of the defects is in the order of 30 ps [23]. Diffusion of these small defects throughout the crystal lattice results in a 180° rotational-C/2 translational (screw-jump) motion of the crystalline stem [24–29]. This screw-jump mechanism is generally accepted as being the molecular origin of the dielectrical α-transition in polyethylene [24–31].

In an unloaded situation, the diffusion of gauche defects will cause translational vibrations within the crystal. Under the influence of stress, this motion can easily induce chain slip, which results in plastic, irreversible deformation of the crystalline material. This view is supported by the value of the apparent activation energy of the plastic flow contribution, approx. 30 kcal/mol, which is identical to the value of the activation energy of the dielectrical α-relaxation [30]. This interpretation is in accordance with the results and conclusions of Wilding and Ward in the case of melt-spun/drawn HDPE fibers [6, 7].

From Fig. 10, it can be observed that plastic deformation causes a significant increase in the tensile modulus. This is not surprising in view of the fact that plastic deformation (creep) is similar to the actual drawing process, albeit on a different time/temperature scale.

Reversible deformation

The molecular interpretation of the reversible (visco-elastic) contribution to the deformation process is rather complex, in contrast to that of the previously discussed plastic flow component. Comparing Figs. 2a and b, one is tempted to conclude that, in view of the similar values of the activation energies at the lower temperature scale (up to appr. 50 °C), the reversible contribution is also related to, or even dominated by translational motions within the crystal, at least at these lower temperatures. The increase in the apparent activation energy of the reversible contribution at the higher temperature scale, Fig. 2a, is generally interpreted in terms of combined contributions of at least two separate, temperature-activated Arrhenius processes for isotropic [32–35] as well as for oriented PE [36–37]. Matsuo et al. [36], for instance, distinguish two separate processes α_1 and α_2 in highly oriented PE, assigned to boundary slip phenomena and a smearing out effect of the crystal lattice potential, due to movement of defects.

However, in Fig. 2a a similarity is observed in the temperature dependence of the dynamic data, measured from 0.2 to 5 Hz (short relaxation times), and stress relaxation data, measured from 100 to 10 000 s (long relaxation times). This similarity suggests that the material behavior is thermorheologically simple, which indicates that a single molecular process is involved. Since this process seemingly does not display an Arrhenius-type behavior, the physical relevance of the apparent activation energies, as derived from Fig. 2a, becomes rather doubtful. Moreover, another relevant issue is that reversible deformation is not compatible with defect diffusion within crystals in view of the irreversible nature of the latter process.

The results concerning volume expansion obtained via dilatometry and WAXS experiments (Fig. 5) support a simple two-phase, crystalline/"amorphous" structure. The "amorphous" component shows a non-linear specific volume increase with increasing temperature, which could be explained in terms of a gradual increase in mobility. The observed reversibility of the volume expansion upon temperature recycling, which implies that $\Delta V \approx 0$ for a cycle of heating and cooling, strongly supports an entropic, rubber-like nature of the "amorphous" material. The entropic effects that are observed upon constrained and unconstrained heating of the fiber (Figs. 6, 7) are consistent with this view.

Taking further into account that the crystalline fraction is already nearly perfectly oriented [10, 11], the observed increase in the sonic and the dynamic moduli upon loading (Figs. 8, 9) is related to further orientation of this "amorphous" fraction.

The NMR data, however, are not in line with

this simple two-phase model [11]. ^{2}H-NMR gave evidence for an amorphous fraction that is oriented to some extent and a highly oriented crystalline fraction [11]. However, considerable molecular mobility was observed for part of the highly oriented, crystalline material. The molecular origin of this motion has been explained in terms of diffusion of gauche defects along a chain. These defects are not homogeneously distributed as T_1-(spin lattice) time sensitive experiments indicated a smooth transition from practically rigid chains to those with about 2% running gauche defects [11].

This complicated microstructure of polyethylene originates from the drawing process, i.e., transformation of folded-chain crystals into oriented/chain-extended structures [38]. During drawing, various conformational defects like chain ends, loops, trapped entanglements, folds, etc. are more or less expelled from the newly formed highly oriented crystalline phase, and become concentrated in the oriented structure, not necessarily in a random manner [39].

Upon loading of this oriented structure, as performed in a creep experiment, the drawing process is in fact continued since there is no basic difference between the actual drawing process and a creep experiment in view of the absence. of any lock-in mechanism during transformation of chain-folded crystals into chain-extended structures. The only difference to the researcher is the time-temperature scale of the experiment. Upon prolonged static loadings, the crystallinity and, hence, the performance of the fiber will increase gradually and irreversibly (see Fig. 10).

The main question which remains is: "what causes the persistent reversible contribution to the deformation behavior of oriented polyethylene systems?"

Based on currently available results of neutron-scattering studies on highly oriented polyethylene systems [40–43], it can be inferred that chains are not perfectly extended. Since the radius of gyration of a polyethylene chain in oriented polyethylene, perpendicular to the drawing direction, is in the range of 20 to 40 Å [42, 43], the root-mean-square deviation of chain segments is in the range of 50 to 100 Å, equivalent to 6–13 units in the a-direction, or 10–20 units in the b-direction of the orthorhombic unit cell. This result implies that a chain will not be in register over its full length, as represented schematically in Fig. 11. Note that the actual chain length in Fig. 11 is at least 100 times larger than schematically drawn for the three chains (based on Mn = approx. 250Kg/mole) and, consequently, register switching as shown in Fig. 11 could occur repeatedly along the chain trajectory.

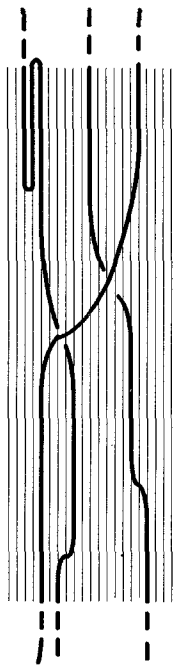

Fig. 11. Schematic representation of the trajectory of some chains in a highly oriented polyethylene structure.

Within the deformation range that is experimentally covered in this study, the entropic contribution of the non-registered chain segments will ensure a persistent reversible contribution to the deformation since chains cannot cross mutually. Only in the limiting case of an infinite draw ratio can a perfect extension of chains be obtained. In practice this will not be realized via tensile drawing.

Conclusion

Based on the combined experimental results presented in this paper, it can be concluded that two separate contributions are operative during deformation of highly oriented polyethylene: an irreversible, plastic flow contribution and a reversible viscoelastic contribution.

The irreversible, plastic flow contribution is related to translational motion of chains within the crystal (chain slip).

The reversible part of the deformation originates from the entropic nature of non-registered chain-segments, which is inherently related to the imperfect extension of chains.

Acknowledgements

The authors wish to thank Prof. Paul Smith (UCSB), Dr. Peter Barham (University of Bristol), and Prof. Martin Möller (University of Twente) for helpful discussions and valuable suggestions. The support of Dr. Manfred Stamm (Max Planck Institut für Polymerforschung, Mainz, Germany) in performing and interpreting the WAXS experiments is gratefully acknowledged. One of the authors (L.G.) is grateful to DSM Research for financial support of this work.

References

1. Barham PJ, Keller A (1985) J Mat Sci 20:2281
2. Ward IM (1985) Adv Polym Sci 70:1
3. Lemstra PJ, Kirschbaum R, Ohta T, Yasuda H (1987) in: Developments in Oriented Polymers 2. Ward IM (ed) Elsevier Appl Sci Publ, New York, Chapter 2
4. Lemstra PJ, van Aerle NAJM, Bastiaansen CWM (1987) Polym J 19:85–98
5. Wilding MA, Ward IM (1978) Polymer 19:969–976
6. Wilding MA, Ward IM (1981) Polymer 22:870–876
7. Wilding MA, Ward IM (1984) J Polym Sci, Polym Phys Ed 22:561–575
8. Govaert LE (1990) PhD-Thesis Eindhoven University of Technology
9. Irvine PA, Smith P (1986) Macromolecules 19:240–242
10. Anandakumaran K, Roy SK, St. John Manley R (1988) Macromol 21:1746
11. Deckmann H, Govaert LE, Möller M, Lemstra PJ (1991) in: Integration of Polymer Science and Technology Part 5:276–290, Elseviers Appl Sci Publ
12. Ciferri A, Ward IM (eds) (1979) Ultra-High Modulus Polymers. Appl Sci Publ England
13. Sherby OD, Dorn JE (1958) J Mech Phys Solids 6:145–162
14. Dent Glasser LS (1977) Crystallography and its applications. Van Nostrand Reinhold Company, pp 142
15. Wilson PS, Simha R (1973) Macromol 6:902–908
16. Carnazzi P (1903) Nuovo Cimento 5:180
17. Northolt MG, Roos A, Kampschreur JH (1989) J Polym Sci, Polym Phys Ed 27:1107–1120
18. Leblans PJR, Bastiaansen CWM, Govaert LE (1989) J Polym Sci, Polym Phys Ed 27:1009–1016
19. Capaccio G, Ward IM (1982) Colloid Polym Sci 260:46–55
20. Decandia F,Vittoria V, Peterlin A (1985) J Polym Sci, Polym Phys Ed 23:1217
21. Smook J (1984) PhD Thesis University of Groningen
22. Khanna YP, Wenner WM, Kumar R, Kavesh S (1989) J Appl Polym Sci 38:571–578
23. Noid DW, Sumpter BG, Wunderlich B (1990) Macromol 23:664
24. Mansfield M, Boyd RH (1978) J Polym Sci, Polym Phys Ed 16:1227–1252
25. Olf HG, Peterlin A (1970) J Polym Sci A-2 8:753
26. Olf HG, Peterlin A (1970) J Polym Sci A-2 8:771
27. Opella SJ, Waugh JS (1977) J Chem Phys 66:4919
28. Reneker DH, Mazur J (1982) Polymer 23:401
29. Ewen B, Strobl TR, Richter D (1980) Faraday Discussions Chem Soc 69:19
30. Boyd RH (1985) Polymer 26:323–347
31. Boyd RH (1985) Polymer 26:1123–1133
32. Nakayasu H, Markovitz H, Plazek DJ (1961) Trans Soc Rheol 5:261–283
33. Kawai H, Hashimoto T, Suehiro S, Fujita K (1984) Polym Eng Sci 24:361
34. Ribes Greus A, Diaz Calleja R (1989) J Appl Polym Sci 37:2549–2562
35. Meier DJ (ed) (1978) Molecular Basis of Transitions and Relaxations. Midland Macromolecular Institute Monographs, No. 4
36. Matsuo M, Sawatari C, Ohhata T (1988) Macromol 21:1317–1324
37. Roy SK, Kyu T, St. John Manley R (1988) Macromol 21:1741–1746
38. van Aerle NAJM, Braam CWM (1988) J Mater Sci 23:4429
39. Kunz M (1990) PhD-Thesis University of Freiburg
40. Sadler DM, Barham PJ (1990) Polymer 31:36–42
41. Sadler DM, Barham PJ (1990) Polymer 31:43–45
42. Sadler DM, Barham PJ (1990) Polymer 31:46–50
43. Stein D (1990) Private Communications

Received April 25, 1991;
accepted July 23, 1991

Authors' address:

Dr. Leon Govaert
Centre for Polymers and Composites
Eindhoven University of Technology
P.O. Box 513
5600 MB Eindhoven, The Netherlands